J Mater Sci (2010) 45:3001–3006
DOI 10.1007/s10853-010-4301-2

Annealing temperature dependence of effective piezoelectric coefficients for $Bi_{3.15}Eu_{0.85}Ti_3O_{12}$ thin films

X. J. Zheng · Q. Y. Wu · J. F. Peng ·
L. He · X. Feng · Y. Q. Chen · D. Z. Zhang

Received: 13 October 2009 / Accepted: 4 February 2010 / Published online: 19 February 2010

Abstract The effects of annealing temperatures 600, 650, 700, and 750 °C on microstructure, chemical composition, leakage current, ferroelectric, dielectric, and piezoelectric properties of $Bi_{3.15}Eu_{0.85}Ti_3O_{12}$ (BET) thin films prepared by metal–organic decomposition were studied in detail. The largest spontaneous polarization $2P_s$ (98.7 μC/cm^2 under 300 kV/cm), remnant polarization $2P_r$ (81.7 μC/cm^2 under 300 kV/cm), dielectric constant ε_r (889.4 at 100 kHz), effective piezoelectric coefficient d_{33} (46.7 pm/V under 260 kV/cm), and lowest leakage current (1.3×10^{-6} A/cm^2 under 125 kV/cm) of BET thin film were obtained with annealing at 700 °C. The mechanisms concerning the dependence of the enhancement d_{33} are discussed according to the phenomenological equation, and the improved piezoelectric performance could make BET thin film a promising candidate for piezoelectric thin film devices.

Introduction

Bismuth (Bi)-layered perovskite lead-free ferroelectric thin films, with the characteristics of larger remnant polarization $2P_r$, fast switching speed, high fatigue resistance with metal electrodes, and good retention, have attracted much attention due to their potential applications in nonvolatile ferroelectric random access memory devices [1]. In the past years, many studies reveal that Bi^{3+} ions in $Bi_4Ti_3O_{12}$ (BIT) structure can be substituted by trivalent lanthanoid ions, such as Nd^{3+}, La^{3+}, Pr^{3+}, Dy^{3+}, and Sm^{3+}, which improves ferroelectric properties [2–4]. In particular, Eu-substituted BIT lead-free thin films have emerged as new ferroelectric materials due to good fatigue endurance and large polarization [5, 6], and in our previous work the $2P_r$ is 82 C/cm^2 for $Bi_{3.15}Eu_{0.85}Ti_3O_{12}$ (BET) lead-free thin film annealed at 700 °C [7]. Recently, more and more efforts have been made to develop nontoxic lead-free piezoelectric materials to apply into piezoelectric microelectromechanical systems (MEMS), and Bi-layered perovskite lead-free ferroelectric thin films are considered to be candidate materials, such as the effective piezoelectric coefficients d_{33} of 30–60 pm/V for $CaBi_4Ti_4O_{15}$ thin films [8, 9], and $\sim$38 pm/V for neodymium-doped $Bi_4Ti_3O_{12}$ (BNT) thin film [10]. According to the phenomenological equation regarding the intrinsic piezoelectric coefficient, the high spontaneous polarization P_s is favorable for yielding higher piezoelectric displacement [10]. It is well known that the annealing temperature has an important effect on the microstructure, dielectric, and ferroelectric properties of Bi-layered perovskite ferroelectric thin films. However, few study has involved the piezoelectric properties of BET thin films annealed at different temperatures, therefore it is imperative for us to improve piezoelectric properties of the thin films in order to impetus for integrating Bi-layered perovskite ferroelectric thin films into MEMS piezoelectric devices.

In this paper, BET lead-free ferroelectric thin films were prepared by metal–organic decomposition (MOD), and the

X. J. Zheng (✉) · Q. Y. Wu · J. F. Peng · L. He ·
Y. Q. Chen · D. Z. Zhang
Faculty of Materials, Optoelectronics and Physics,
Xiangtan University, Xiangtan 411105, Hunan,
People's Republic of China
e-mail: zhengxuejun@xtu.edu.cn

X. J. Zheng · L. He
Key Laboratory of Low Dimensional Materials and Application
Technology of the Ministry of Education, Xiangtan University,
Xiangtan 411105, Hunan, People's Republic of China

X. Feng
School of Aerospace, Tsinghua University, Beijing 100084,
People's Republic of China

effects of annealing temperature on microstructure, chemical composition, leakage current, ferroelectric, dielectric, and piezoelectric properties were investigated by field emission scanning electron microscopy (FE-SEM), X-ray diffraction (XRD), Raman spectrometer, energy dispersive X-ray spectroscopy (EDS), semiconductor characterization system, ferroelectric tester, impedance analyzer, and scanning probe microscope (SPM). The ferroelectric, dielectric, leakage current, and piezoelectric behaviors were established from polarization–electric field (P–E) hysteresis loops, dielectric constant–frequency (ε_r–f) and dissipation–frequency ($\tan\delta$–f) curves, current density–electric field (J–E) curves, and displacement–electric field (D–E) "butterfly" curves, respectively. We expect that the research can offer useful guidelines to the design of Bi-layered thin film piezoelectric devices.

Experimental details

Preparation of sample

BET thin films were deposited on Pt(200 nm)/Ti(30 nm)/SiO_2/Si(111) substrate by MOD method [5, 6]. The precursor materials were bismuth (III) acetate $\{Bi[CH_3CO_2]_3\}$, europium (III) acetate hydrate $\{Eu[CH_3CO_2]_3\}$, and tetrabutyl titanium $\{Ti[OC_4H_9]_4\}$, and the solvents were acetic acid $\{CH_3CO_2H\}$ and acetylacetone $\{CH_3COCH_2COCH_3\}$. A 10% excess amount of bismuth acetate was used to compensate Bi-loss during annealing process. At first, the solid-state bismuth acetate and europium acetate were dissolved in the acetic acid, and the solution was mixed to obtain the (Bi, Eu) stock solution followed by stirring for 12 h. Second, the tetrabutyl titanium was dissolved in the mixture of the stock solution and acetylacetone, and it was magnetically stirred in the air atmosphere for 1 h. Finally, the flaxen, transparent and stable BET precursor solution was prepared. The precursor solutions with a mole ratio (Bi:Eu:Ti) of 3.465:0.85:3 were spun on the substrate at 4000 rpm for 30 s. After the spin-coating procedure, the thin films were kept in rapid temperature process at 400 °C for 180 s to remove the organic ingredients. The coating/drying circles were repeated seven times to achieve desired film thickness, and the pre-baked films were, respectively, annealed at 600, 650, 700, and 750 °C in an oxygen atmosphere to promote crystallization.

Characterization methods

Using FE-SEM (1525, LEO, Germany), the surface morphologies of BET thin films were identified with 50 K amplificatory, and the cross-sectional micrograph of BET thin film annealed at 700 °C was recorded with 20 K amplificatory. The chemical composition analysis was investigated by EDS (INCA, Oxford, England), and the incoming energy of the EDS electron beam was 20 kV. Phase identification, degree of crystallinity, and crystalline orientation of the thin films were investigated by XRD (X'Pert PRO, PANalytical, Netherlands) using the normal scanning method, and they were scanned at 10°/min with Cu radiation (40 kV, 30 mA). The Raman spectroscopy was performed using the Raman spectrometer (Model 3000, Reinishaw, England). The backscattering configuration was employed. The Argon ion laser beam of 514.5 nm wavelength with a power of 0.5 mW was focused on a 1 mm spot on the middle of BET thin films. The circular Au top electrodes with radius of 0.1 mm were deposited on the thin films using a shadow mask by dc magnetron sputtering, and under the electric field 300 kV/cm the P–E hysteresis loops were measured by ferroelectric tester (Precision Workstation, Radiant Technologies, USA). Frequency dependent dielectric constant (ε_r) and dissipation factor ($\tan\delta$) were measured by the impedance analyzer (HP4194A, Hewlett Packard, America). The leakage current properties were measured by the semiconductor characterization system (4200-SCS, Keithly, America) at applied voltage of 0–5 V. A commercial available SPM (SPI4000&SPA300HV, Seiko, Japan) was used to characterize piezoelectric properties of the thin films without top electrode. The conductive rhodium coated silicon cantilever is of a spring constant of 1.9 N/m, a resonant frequency of 28 kHz, and an integrated tip of about 10 nm in diameter. The stiff cantilever was used to get a large indentation force ensuring that the measurement was in the so-called strong-indentation regime [11]. The piezoelectric measurement was conducted on 10 points of scanned scope on the sample surface, because the piezoelectric characterization for SPM is a kind of local method [12]. For each sample, keeping the SPM tip fixed above the interesting point the D–E "butterfly" curve was recorded under a dc voltage applied from −9 to 9 V. With considering the unexpected shift of the intersection from the origin of D–E curve, the d_{33}–electric field (d_{33}–E) loops can be calculated according to the modified equation of converse piezoelectric effect [12]

$$d_{33} = \frac{D - D_I}{d(E - E_I)}, \tag{1}$$

where d is the initial film thickness before deformation. On the D–E curve, D_I and E_I are the piezoelectric displacement and electric field for the intersection, and D and E are the measured values of piezoelectric displacement and electric field for each point. All of the above measurements were carried out at room temperature.

Results and discussion

Surface and interfacial profiles

The surface micrographs of BET thin films annealed at 600, 650, 700, and 750 °C are given in Fig. 1a–d, and the typical cross-sectional micrograph of the thin film annealed at 700 °C is described as Fig. 1e. In Fig. 1a–d, there are a few pinholes and voids on the film surfaces but crack-free, and the grain sizes of BET thin films annealed at 600, 650, 700, and 750 °C are about 106, 178, 241, and 306 nm, respectively. With the increase of annealing temperature, the pinholes and voids decrease and the grain sizes enlarge, indicating that the high annealing temperature enhances the crystal growth. The crack-free surface seems to be important for ferroelectric thin films because the crack will affect the microstructure, ferroelectric properties, and residual stress [13]. From Fig. 1e, the multiple-layers structure is obviously observed for BET thin film annealed at 700 °C, and the thickness is uniformity 350 nm, which implies a coating/drying cycle about 50 nm. The density is very crucial for MEMS application.

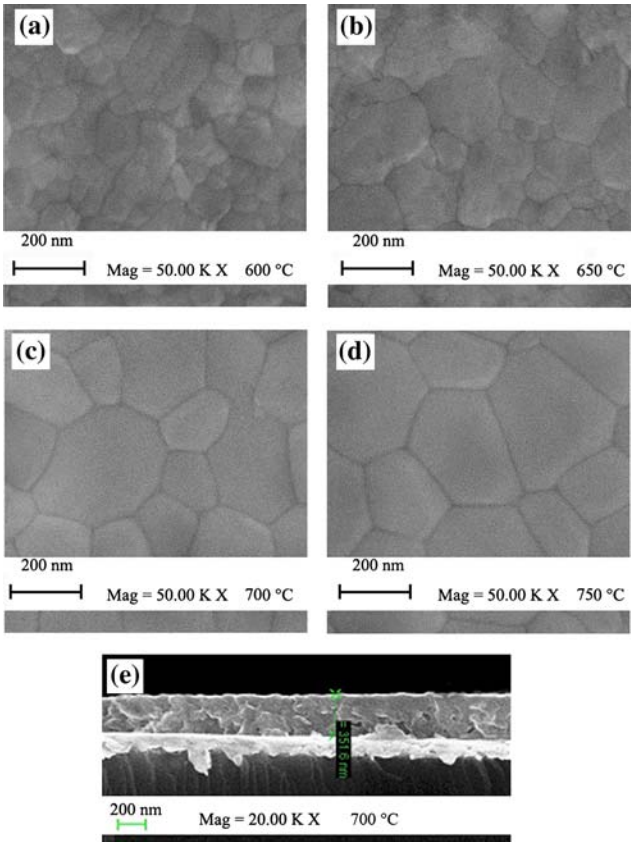

Fig. 1 The surface morphologies of BET thin films annealed at **a** 600, **b** 650, **c** 700, **d** 750 °C, and **e** a cross-sectional micrograph for the thin film annealed at 700 °C

Crystalline structure

A typical EDS spectrum of BET thin film annealed at 700 °C is given in Fig. 2a, and Ti, Bi, O, Eu, Pt, and Si peaks are detected, obviously. Ti, Bi, and O peaks as well as Eu peaks originate from BET thin film, while Pt and Si peaks originate from the substrate. To understand the effect of annealing temperature on Bi^{3+} ions volatile quantity, the collected elemental composition data of BET thin films annealed at 600, 650, 700, and 750 °C are summed up as Fig. 2b. Bi atomic mol ratios are estimated as 15.23, 15.11, 12.28, and 8.77% for BET thin films annealed at 600, 650, 700, and 750 °C, respectively. Bi^{3+} ions volatile quantity increases with the annealing temperature, and it enhances sharply for BET thin film annealed at 750 °C. Eu atomic mol ratios in BET thin films are estimated about 4.43%, and it indicates that the substitution of Eu^{3+} to Bi^{3+}occurs successfully. Figure 3a shows typical Bi-layered perovskite polycrystalline phase without any pyrochlore phase and other phases related to Eu, and it indicates that the substitution of Eu^{3+} to Bi^{3+}occurs successfully [5], and it is consistent with EDS result given in Fig. 2b. At 600 °C, the diffraction peaks are low and broad, indicating poor crystallinity of the sample. With the increase of annealing temperature, the diffraction peaks become sharp and strong, indicating the possible improved crystallinity. According to $(I_{(006)} + I_{(008)} + I_{(0016)})/\Sigma I_{hkl} \times 100\%$ (where I_{hkl} is the relative intensity of the corresponding peak) [14], the degrees of *c*-axis orientation are 28.8, 41.9, 45.0, and 47.1% for BET thin films annealed at 600, 650, 700, and 750 °C, respectively. It indicates the degree of *c*-axis orientation of BET thin films increases with annealing temperature. Figure 3b shows Raman spectroscopy of BET thin films annealed at 600, 650, 700, and 750 °C. The peak centered at 261 cm^{-1} corresponds to the TiO_6 octahedron torsional bending mode, which is representative of the pseudo-perovskite structure in BET thin films, and the peaks centered at 562^{-1} and 848 cm^{-1} are related to the TiO_6 stretching mode. The intensity and sharpness of the three peaks increase with the annealing temperature, indicating improvement in crystalline quality of the perovskite structure, and it is consistent with XRD results given in Fig. 3a. The peak centered at 321 cm^{-1} corresponds to the combination of stretching and bending of the TiO_6 octahedron, and becomes sharper and more distinct with the increase of annealing temperature. The change of TiO_6 mode is most probably due to exaggerations of orthorhombic distortion and octahedral tilting at higher annealing temperature [6, 15].

Dielectric and loss properties

From the ε_r–f and $\tan\delta$–f curves shown as Fig. 4a, under the applied frequency from 1 kHz to 1 MHz, the ε_r values

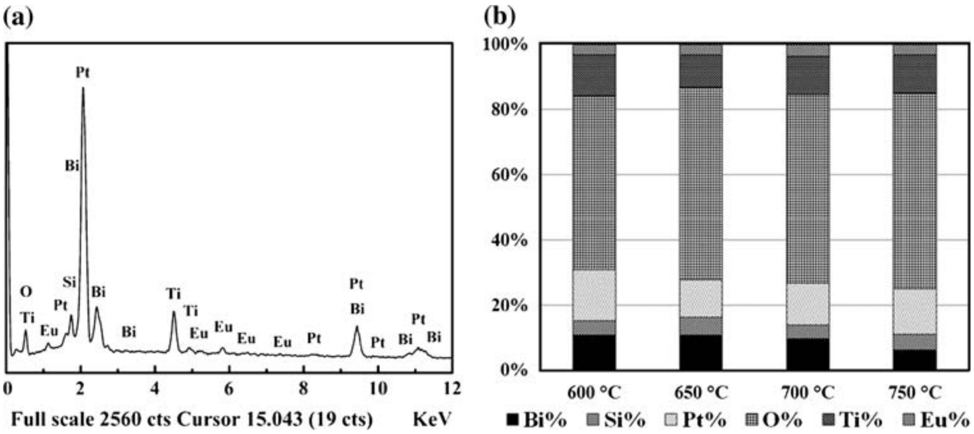

Fig. 2 **a** The typical EDS spectrum of BET thin film annealed at 700 °C and **b** EDS elemental composition of BET thin films annealed at 600, 650, 700, and 750 °C

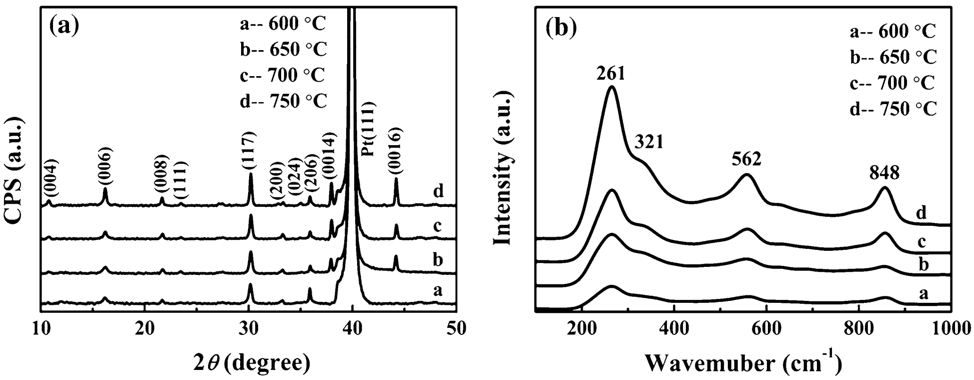

Fig. 3 X-ray diffraction patterns (**a**) and Raman spectroscopy (**b**) of BET thin films annealed at 600, 650, 700, and 750 °C, respectively

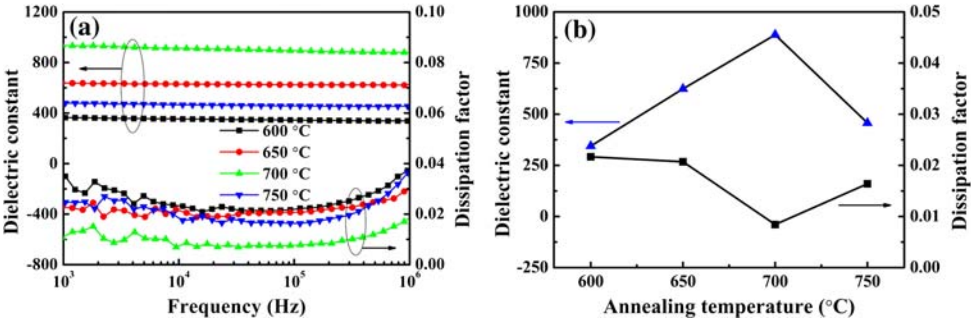

Fig. 4 **a** Frequency dependent ε_r and tanδ of BET thin films annealed at 600, 650, 700, 750 °C, and **b** at 100 kHz the ε_r and tanδ as function of annealing temperature

decrease with the increase of frequency, and it is due to an extrinsic resonance behavior resulting from the microstructure deficiency, which may in principle be reduced by optimization of the film growth process [16]. The tanδ increases at higher frequencies, and the increasing tendency of tanδ is also reported for BNT and $Bi_{3.25}La_{0.75}Ti_3O_{12}$ (BLT) ferroelectric thin films [17, 18]. There are three possible reasons for the dispersion as follows. One possible cause is the extrinsic resonance behavior which results from the microstructure deficiency [16]. Another one is the resistive losses, because the mobile charges contained in the film cannot follow higher frequency electric fields [19]. The third one is the hypothesis of the influence of the contact resistance between the probe and the electrode [17]. Figure 4b shows ε_r and tanδ as function of annealing temperature at 100 kHz, and the values of ε_r and tanδ were estimated as 344.6, 624.2, 888.3, 457.0, and 0.022, 0.021, 0.008, 0.016 for BET thin films annealed at 600, 650, 700, and 750 °C, respectively. Obviously, the ε_r increases with annealing temperature at the range from 600 to 700 °C, while decreases from 700 to 750 °C. The possible reason is the grain size effect on dielectric properties of polycrystalline thin films for the former, and the other is the insufficient Bi supply in Fig. 2b which results in non-stoichiometric structural defects in the thin films for the latter. The tanδ decreases with annealing temperature at the range from 600 to 700 °C, while increases from 700 to 750 °C. It is mainly dominated by mobile charges in the film, such as oxygen vacancy [20, 21], and the annealing temperature may also affect the oxygen vacancies which lead to the decrease in tanδ for BET thin films annealed from 600 to 700 °C. At the annealing temperature of 700–750 °C, the tanδ value increases due to the insufficient Bi supply as shown as Fig. 2b.

Polarization, piezoelectric response, and leakage current

The *P*–*E* loops of BET thin films annealed at 600, 650, 700, and 750 °C are shown in Fig. 5a, the leakage current densities versus the applied electric field of Au/BET/Pt capacitors are exhibited in Fig. 5b, and the typical *D*–*E* (black) curve and d_{33}–*E* (blue) loop are given in Fig. 5c. From Fig. 5a, under the applied field of 300 kV/cm, the values of $2P_s$ and $2P_r$ are 47.9, 66.2, 98.7, 77.4 C/cm^2 and 35.5, 55.7, 81.7, 64.0 C/cm^2 for BET thin films annealed at 600, 650, 700, and 750 °C, respectively. With the increase of annealing temperature the values of $2P_r$ and $2P_s$ increase at the range from 600 to 700 °C while decrease from 700 to 750 °C. It is in a good agreement with the previous result that the $2P_r$ of BET thin film annealed at 700 °C is 82 C/cm^2 [7]. There is more than one contributor causing opening of the hysteresis loops at zero field observed in Fig. 5a, which is a common phenomenon for ferroelectric thin films. It is very likely due to incomplete domain back-switching in association with slow domain wall motion arising from pinning by defects such as oxygen vacancies [22]. The leakage current densities of BET films annealed at different temperatures are shown in Fig. 5b, and they are 4.25, 1.82, 1.30, and 2.23 × 10^{-5} A/cm^2 at 125 kV/cm for BET films annealed at 600, 650, 700, and 750 °C, respectively. From 600 to 700 °C, it appears obvious that the change in morphology (see Fig. 1a–c) with increasing temperature is responsible for the decrease in leakage current in Fig. 5b, and it is in agreement with the previous results [23]. The higher the annealing temperature is, the fewer the dislocations and vacancies that result in degradation of conductivity [24]. Therefore, the leakage current density decreases with the increase of annealing temperature. However, from 700 to 750 °C the leakage current density dramatically rises due to the insufficient Bi supply [23] as shown as Fig. 2b. In Fig. 5c, the d_{33}–*E* loop is almost symmetric and it is in an agreement with the previous symmetries of BiScO$_3$–PbTiO$_3$ and Zn$_{1-x}$V$_x$O ferroelectric thin films [12, 25]. On the *D*–*E* curve, there is no notable horizontal shift, and little vertical shift 0.07 nm can be observed, indicating no obvious imprint effect. The d_{33}–*E* loop clearly shows that BET thin film is switchable and the piezoelectric is retained [26]. Under a bias field of 260 kV/cm, the typical value of d_{33} is 49.9 pm/V for BET thin film annealed at 700 °C, and the average values of d_{33} are 29.1, 37.5, 46.7, and 30.2 pm/V for the BET thin films annealed at 600, 650, 700, and 750 °C, respectively. The d_{33} 46.7 pm/V is larger than 19 pm/V for BLT thin film and 38 pm/V for BNT thin film [10], and it is comparative with 40–110 pm/V for PbZr$_x$Ti$_{1-x}$O$_3$ (PZT) thin films [27, 28]. It is safe to say that the d_{33} value stands in comparison with PZT thin films, therefore BET thin films can be considered as a viable alternative to PZT thin films for selected applications.

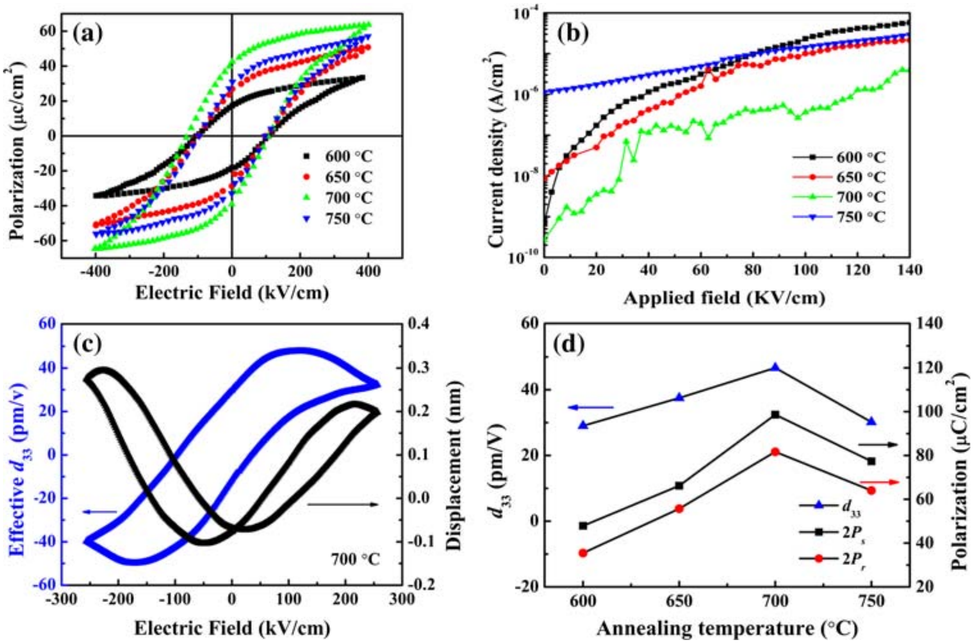

Fig. 5 **a** *P*–*E* hysteresis loops of BET thin films annealed at 600, 650, 700, 750 °C, and **b** *J*–*E* characteristics for BET thin films, **c** representative *D*–*E* curve, d_{33}–*E* loop of BET thin film annealed at 700 °C and **d** $2P_s$, $2P_r$, and d_{33} of BET films as function of annealing temperature

Annealing temperature dependence of piezoelectric responses

The average values of $2P_r$, $2P_s$, and d_{33} as the function of annealing temperature are shown in Fig. 5d. One can read that with increase of annealing temperature all of $2P_r$, $2P_s$, and d_{33} increase at the range from 600 to 700 °C while decrease from 700 to 750 °C. For BET thin films annealed at 600–700 °C, the surface morphologies in Fig. 1a–c, degree of crystallinity and *c*-axis orientation in Fig. 3a are improved, while the leakage current decreases as shown in Fig. 5b with the increase of annealing temperature. Therefore, $2P_r$ and $2P_s$ increase at the range from 600 to 700 °C [29]. For BET thin film annealed at 750 °C, there is excessive volatile of Bi as shown in Fig. 2b, and the leakage current density dramatically rises as shown in Fig. 5b. Therefore, $2P_r$ and $2P_s$ of BET thin film annealed at 750 °C are lower than those annealed at 700 °C. Obviously, the variation of ε_r with annealing temperature is similar with those of $2P_r$ and $2P_s$ as shown as Fig. 4b. The d_{33} can be expressed by the phenomenological equation for most ferroelectric materials [30]

$$d_{33} = 2Q_{\mathrm{eff}}\varepsilon_0\varepsilon_r P_s \tag{2}$$

where Q_{eff} is the effective electrostriction coefficient, ε_0 and ε_r are the permittivity of free space and relative permittivity. Because Q_{eff} is less sensitive to film quality than d_{33} [31], ε_r and P_s can be regarded as the primary factors to relate with d_{33}. The d_{33} variation with annealing temperature should be monotonically corresponding to those of ε_r and P_s, therefore the dependence of d_{33} on annealing temperature should be as same as those of ε_r and P_s in Figs. 4 and 5 for the orientation direction, crystallinity, leakage, and chemical composition of the thin films. Obviously, BET thin film annealed at 700 °C is of the lowest leakage current density and dielectric loss, the highest dielectric constant and effective piezoelectric coefficient, implying that it is suitable for use as ferroelectric capacitors [32].

Conclusions

In conclusion, the average d_{33} of BET thin film annealed at 700 °C is 46.7 pm/V under the bias field 260 kV/cm, and it is larger than that of the others. With the increase of annealing temperature, the $2P_s$, $2P_r$, ε_r and d_{33} values obviously increase at the range from 600 to 700 °C while decrease from 700 to 750 °C. The leakage current density and the dielectric loss decrease with the increase of annealing temperature from 600 to 700 °C, while increase with from annealing temperature 700 to 750 °C. The d_{33} variation may contribute to the annealing temperature dependence of P_s and ε_r for BET thin film. The improved piezoelectric properties could make Eu-doped BIT a promising candidate for sensors, actuators, and transducers.

Acknowledgements This work was supported by NNSF of China (10672139, 10825209, 50872117), Changjiang Scholar Incentive Program ([2009]17) and Project of Hunan's Prestigious Fu-rong Scholar Award ([2007]362).

References

1. Funakubo H, Watanabe T, Kojima T, Sakai T, Noguchi Y, Miyayama M (2003) J Cryst Growth 248:180
2. Lee HN, Hesse D, Zakharov N (2002) Science 296:2006
3. Chon U, Yi GC, Jang HM (2001) Phys Rev Lett 78:658
4. Chon U, Shim JS, Jang HM (2003) J Appl Phys 93:4769
5. Kima WJ, Kima SS (2004) J Cryst Growth 262:327
6. Lim KT, Kim KT (2004) Thin Solid Films 447:337
7. Zheng XJ, He L, Zhou YC, Tang MH (2006) Appl Phys Lett 89:252908
8. Kato K, Fu D, Suzuki K, Tanaka K, Nishizava K, Miki T (2004) Appl Phys Lett 84:3771
9. Simões AZ, Ramírez MA, Ries A, Varela JA, Longo E, Ramesh R (2006) Appl Phys Lett 88:072916
10. Maiwa H, Iizawa N, Togawa D, Hayashi T, Sakamoto W, Yamada M, Hirano SI (2003) Appl Phys Lett 82:1760
11. Kalinin SV, Bonnell DA (2002) Phys Rev B 65:125408
12. Yang YC, Song C, Wang XH, Zeng F, Pan F (2008) Appl Phys Lett 92:012907
13. Osada M, Tada M, Kakihana M, Watanabe T (2001) Jpn J Appl Phys Part 1 40:5572
14. Cho CR, Lee WJ, Yu BG, Kim BW (1999) J Appl Phys 86:2700
15. Chu MW, Ganne M, Caldes MT (2002) J Appl Phys 91:3178
16. Guo YP, Akai D, Sawada K, Ishida M (2008) Solid State Sci 10:928
17. Zhong XL, Wang JB, Yang SX, Zhou YC (2006) Appl Surf Sci 253:417
18. Zhong XL, Wang JB, Liao M, Tan CB, Shu HB, Zhou YC (2008) Thin Solid Films 516:8240
19. Jiang H, Hong LG, Venkatasubramanian N, Grant JT, Eyink K, Wiacek K, Fries-Carr S, Enlow J, Bunning TJ (2007) Thin Solid Films 515:3513
20. Ye Y, Guo TL (2009) Ceram Int 35:2761
21. Tsai MS, Sun SC, Tseng TY (1997) J Appl Phys 82(7):3482
22. Zhou ZH, Xue JM, Li WZ, Wang J, Zhu H, Miao JM (2004) Appl Phys Lett 85:804
23. Zheng XJ, Yi WM, Chen YQ, Wu QY, He L (2007) Scripta Mater 57:675
24. Moert M, Schindler G, Mikolajick T, Nagel N, Hartner W, Dehm C, Kohlstedt H, Waser R (2005) Appl Surf Sci 249:23
25. Wen H, Wang XH, Zhong CF, Shu LK, Li LT (2007) Appl Phys Lett 90:202902
26. Yang YC, Song C, Wang XH, Zeng F, Pan F (2008) J Appl Phys 103:074107
27. Muralt P (2000) IEEE Trans Ultrason Ferroelectr Freq Control 47:903
28. Kholkine AL, Wütchrich C, Taylor DV, Setter N (1996) Rev Sci Instrum 67:1935
29. Chon U, Jang HM, Kim MG, Chang CH (2002) Phys Rev Lett 89:087601
30. Kholkin AL, Akdogan EK, Safari A, Chauvy PF, Setter N (2001) J Appl Phys 89:8066
31. Hosono Y, Harada K, Yamashita Y (2001) Jpn J Appl Phys 40:5722
32. Kuh BJ, Choo WK (2001) J Eur Ceram Soc 21:1509